

Article

Insights into Plugging of Pipe Piles Based on Pile Dimensions

Antonio Kodsy  and Magued Iskander * 

Civil and Urban Engineering Department, Tandon School of Engineering, New York University,
New York, NY 11201, USA; kodsy@nyu.edu

* Correspondence: iskander@nyu.edu

Abstract: Preliminary identification of plugging of open-ended pipe piles based on their dimensions, ahead of driving, is explored in this study using data analytics. Piles can be unplugged, plugged, or internally plugged, depending on their dimensions, and geotechnical conditions. Plugging of pipe piles influences both pile capacity and driving behavior; however, the classification assumed at the design time does not always manifest during driving, sometimes resulting in driving difficulties. The relationship between pile plugging and pile dimensions was investigated using a dataset of 74 load tests on pipe piles, where geotechnical profiles were also available. An analytics approach borrowed from data science was adopted. First, capacity was computed using four recognized designed methods considering the unplugged, plugged, and internally plugged conditions. Next, the calculated capacities were compared to capacities measured (interpreted) from static load tests. Finally, voting was employed to identify plugging based on the closeness of the computed capacity assumptions to the interpreted capacity. Most piles were found to be unplugged. A diameter criterion is proposed as a tool to give early insight into the plugging condition of a pile ahead of driving which resulted in a $70 \pm 10\%$ accuracy. The proposed criterion was validated once using a dataset of 23 piles with CPT data and a second time using 24 published driving records where plugging records were available and achieved similar accuracy, in both cases. It was concluded that piles larger than ~ 0.9 m (36 inches) in diameter have a higher likelihood of being unplugged, while piles smaller than 0.5 m (20 inches) have a higher likelihood of being plugged.



Citation: Kodsy, A.; Iskander, M. Insights into Plugging of Pipe Piles Based on Pile Dimensions. *Appl. Sci.* **2022**, *12*, 2711. <https://doi.org/10.3390/app12052711>

Academic Editor: Roohollah Kalatehjari

Received: 9 February 2022

Accepted: 2 March 2022

Published: 5 March 2022

Publisher's Note: MDPI stays neutral with regard to jurisdictional claims in published maps and institutional affiliations.



Copyright: © 2022 by the authors. Licensee MDPI, Basel, Switzerland. This article is an open access article distributed under the terms and conditions of the Creative Commons Attribution (CC BY) license (<https://creativecommons.org/licenses/by/4.0/>).

Keywords: deep foundation; resistance; L/D ratio; length; diameter; data-driven decisions; data science; data analytics

1. Introduction

Pipe piles are routinely used to support a variety of structures ranging from residential and commercial structures to infrastructure projects. As a result, and due to the vast differences in soil conditions, these piles are used with a wide range of diameters and lengths. During installation of open-ended pipe piles, initially, the pile penetrates the soil in a *coring* mode where the soil enters the pile at an equal or higher rate to the rate of pile penetration. As penetration advances, the pile may become plugged if the soil core inside the pile develops ample frictional resistance along the inner pile wall, impeding further soil incursion inside the pile. Technically, the soil *core* is typically referred to as a “*plug*” only when it is wedged against the pile, thus preventing any additional soil entry into the pile. Unfortunately, the term plug has often been used to refer to the core regardless of its state during installation [1].

The driving response of piles is affected by the plugging condition [2], which makes their dynamic analyses more intricate [3]; however, plugging is perhaps more crucial since it directly contributes to the end bearing capacity of the pile. In addition, plugged piles displace more soil than unplugged piles, which consequently increases the effective stresses around the pile [4], thus indirectly contributing to the shaft capacity.

Generally, the majority of piles that experience plugging during static loading do not plug during driving [5]. This could be attributed to a combination of an increase in

the bearing capacity factor, N_q , over its static value due to inertial effects [6]; moreover, Smith et al. [7] claimed that the internal and external friction of a driven pile is mobilized intermittently during penetration, and therefore, the soil core advances up the pile. Contrarily, Paikowsky et al. [8] argued that during driving, “the pile plugging phenomenon is of frequent occurrence and is of greater significance than that presently accorded it by the profession”. Nevertheless, the plugging degree relies on the soil properties, pile dimensions, the pile’s frictional resistance, the driving hammer characteristics, and the plug drainage conditions [9,10]. The ability of the plug to resist the applied loads depends on whether these loads are static, cyclic, or seismic [11].

On some occasions, a situation may arise where the available pile driving hammer cannot drive the pile to the design depth, which could stem from the pile being plugged and impeding the driving. The problem is more critical for piles used to resist lateral loading, or more generally, piles with thickened walls near the surface [12]. The installation technique used can also impact the plugging of the piles [13]. Henke and Grabe [14] suggested that piles installed using dynamic methods, such as vibratory driving or impact driving, exhibit less plugging compared to jacked piles. They later showed that piles installed using impact driving also exhibit plugging [15], in contradiction with the earlier findings of Randolph [16] who concluded that no soil plug is formed inside impact-driven open-ended piles and attributed that to the inertia of the soil column inside the pile. If a plug forms during pile installation, the plug may be removed by drilling or jetting; however, this negatively affects the axial capacity and is therefore undesirable.

The effects of the soil plug removal on the final pile capacity are controversial. Bruzy et al. [17] claimed that static loading results remain unchanged by partially removing the soil plug. Other studies have shown that, even if the pile is re-driven, a significant reduction in the overall pile capacity results from jetting [18]. More recent studies also show that removing the plug decreases the pile capacity by 45% to 79% in sand specifically [19]. Therefore, it is necessary to understand the conditions that may lead to plugging, in order to avoid them; or to have an appropriate hammer available to drive the pile to the required depth.

Pile plugging could be quantified using the Incremental Filling Ratio (IFR), which represents the amount of soil plugging in a pile, or the Plug Length Ratio (PLR), which is a global indicator of pile plugging, that is easier to measure at the end of driving [20]. IFR and PLR are not necessarily correlated, especially because IFR can change rapidly from near zero to much greater values, or vice versa, while the PLR remains largely unchanged [21]. Methods to predict and account for pile plugging on capacity based on the IFR and PLR have been proposed by Paik and Salgado [3], Yu and Yang [22], and Jeong et al. [23]. In addition, methods to predict the contribution of the plug to the pile capacity have also been developed [24,25]; however, the required information is typically not available during initial design required to size piles.

The relationship between pile plugging and geometrical properties of the pile such as diameter (D), length (L), and L/D was also explored. The occurrence of plugging was identified using load test data. Interpreted (measured) capacities are compared to the computed capacities for the three plugging conditions: (1) Plugged, (2) Unplugged, and (3) Internal Plugged. The plugging condition during loading is assumed to be that which corresponds to the calculated capacity from one of the three aforementioned conditions and is closest to the interpreted capacity.

This study employs data-driven decisions to identify plugging. In the past, other studies have employed experimental and theoretical approaches and the matter remains unresolved, thus we employed tools of data science. The onset of plugging is identified by comparing the measured (i.e., interpreted) pile capacity to that obtained from static analyses; however, there is a great difference between the pile capacities computed with the many available design methods. Therefore, four commonly used design methods were employed, and the analysis was repeated separately for each design method. Next, the plugging condition is identified via simple voting from the four methods. Finally, a methodology is

proposed to forecast the plugging condition of a pile based on its geometrical dimensions in an effort to shed some light on the pile plugging phenomenon.

2. Load Test Data

A dataset of 74 piles compiled from the FHWA *Deep Foundation Load Test Database* (DFLTD) v.2 [26] and Olson's Database [27–30] was employed in this study. Dimensions of piles employed for analysis along with associated soil conditions are summarized in Appendices A and B, for DFLTD and Olson databases, respectively. These load tests were ported to a relational database for easy access [31]. The scope of this paper was limited to statically loaded steel pipe piles and hollow concrete piles with ample soil profile data for capacity calculations (Q_c), and interpretable compression load tests for capacity measurement (Q_m). The piles ranged between 0.25–2.54 m (10–100 in) in diameter and 7.5–113 m (24.6–370 ft) in length. The distribution of the diameter and length of the studied piles is shown in Figure 1. A summary of the bearing layer of the piles in the dataset is also shown in Figure 1, showing that nearly 65% of the pile toes employed in this study bear in sand, while approximately 35% bear in clay. All load tests were carried in compression according to ASTM D1143 [32], but information regarding the time duration between installation and load testing was not always available.

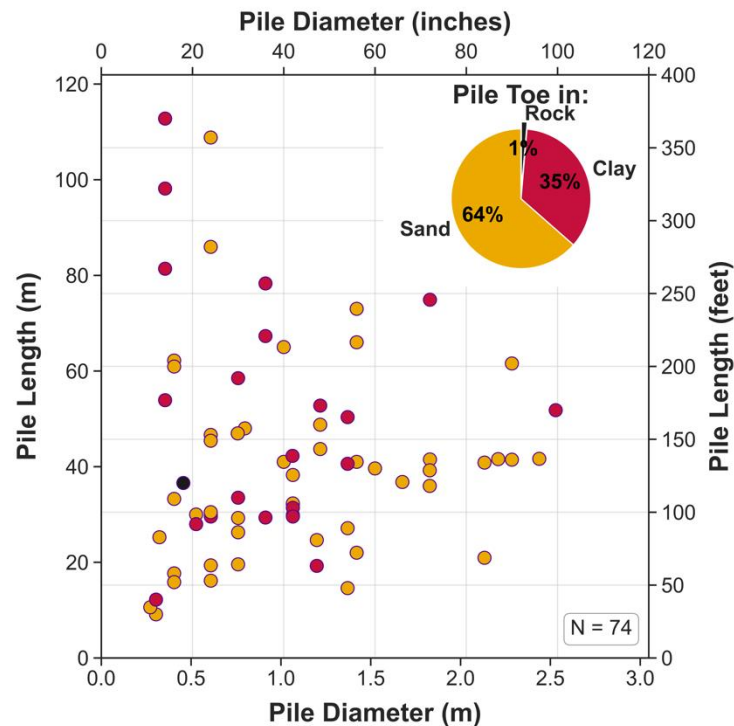


Figure 1. Distribution of pile diameter and length of load tests employed in this study. The distribution of the bearing layer is also depicted in the top right.

Missing or misinterpreted data is one of the dominant issues when dealing with geotechnical databases. Therefore, all the soil data associated with the chosen piles were reviewed by the research team to check its integrity and usability. Available geotechnical design parameters were employed to compute Q_c where possible, but many pile cases lacked sufficient measurements, so the team used empirical relationships from established guidelines such as those provided by The Naval Facilities Engineering Command Design Manual 7.01 [33] and Peck et al. [34] to supplement laboratory data. More details about data handling are available in Rizk et al. [35].

3. Plugging and Capacity

The ultimate bearing capacity of the pile (Q_c) is typically calculated by adding the shaft resistance R_s , and the toe resistance R_p . Open-ended piles experience one of three possible plugging conditions: (i) unplugged, (ii) plugged, or (iii) internal plug. Designers are typically unable to predict which condition will prevail, and thus check all conditions and adopt the minimum capacity as a conservative approach. Paikowsky and Whitman [20] presented equations to calculate the pile capacity if the pile is plugged (Equation (1)) or if the pile is partially plugged or unplugged (Equation (2)).

$$Q_c = \sum f_{so} A_{so} + q_p A_{pp} - W_p \quad (1)$$

$$Q_c = \sum f_{so} A_{so} + \sum f_{si} A_{si} + q_p A_p - W_p \quad (2)$$

where f_{so} is the exterior unit shaft resistance, A_{so} is the pile exterior surface area, q_p is the unit toe resistance, A_{pp} is the cross-sectional area of the pile and soil plug at pile toe ($\frac{\pi D^2}{4}$), D is pile outer diameter, f_{si} is the interior unit shaft resistance, A_{si} is the pile interior surface area, A_p is the pile toe cross-sectional area ($\frac{\pi(D^2 - D_i^2)}{4}$), D_i is pile inner diameter and W_p is the weight of the pile and soil plug.

In the unplugged condition, the pile is assumed to behave as a “cookie-cutter” coring through the soil without exhibiting internal friction. The pile capacity is the summation of exterior skin friction and end bearing of the pile annulus section (i.e., f_{si} in Equation (2) is taken as 0). For the plugged condition, the pile is assumed to behave as a full displacement pile and hence the capacity is the summation of exterior skin friction and end bearing of the entire toe area (Equation (1)). Finally, in the internal plug condition, it is theorized that the pile might experience interior skin friction. The capacity is taken as the summation of exterior skin friction and the lesser of: (1) the end bearing of the entire toe area; or (2) the end bearing of the pile annulus section plus the interior skin friction. Interior skin friction (f_{si}) is typically taken as 40% of the exterior skin friction (f_{so}) in cohesive soils, and as 100% of the exterior skin friction in cohesionless soil ($f_{si} = f_{so}$) [36].

4. Pile Design Methods Employed for Identification of Plugging

Four classic design methods are implemented in this study for the purpose of computing the capacity (Q_c), namely: (1) United States Federal Highway Administration, FHWA [36]; (2) United States Army Corps of Engineers [37]; (3) Revised Lambda [38,39]; and (4) American Petroleum Institute [40]. These four methods were chosen for their wide acceptance and use by many institutions and engineering firms. Many of the design methods have well-recognized limitations, which may potentially be addressed through stochastic analysis; however, this is beyond the scope of this work. This study is addressed primarily to practicing engineers, and therefore focuses on using the available design methods and design tools. Comprehensive description of these design methods can be found in Reese et al. [41], Hannigan et al. [36], or Wang et al. [42]. Note that more recent design methods require the use of CPT data, which were not available for the majority class of the data. Thus, these four classic methods were used to develop the methodology and for CPT methods were used for validation. The following is a brief description of the similarities and difference between the methods.

4.1. Federal Highway Administration (FHWA) Method

For piles smaller than 18 inches in diameter, the FHWA recommends using the α -method [43] for cohesive soils and the Nordlund method [44] for cohesionless soils. The α -method applies α reduction factors that are directly proportional to the undrained shear strength (s_u) for cohesive soil to calculate the adhesion between the pile side and the surrounding soils. It also provides other reduction factors to account for drag-down, a phenomenon that occurs during pile driving in mixed soil profiles and results in a side resistance reduction. For the cohesionless soils, the Nordlund method, detailed in

Hannigan et al. [36], uses several complex charts to account for the effects of pile type, taper, slenderness ratio, material, friction angle, and soil displacement to acquire the design parameters.

4.2. United States Army Corps of Engineers (USACE) Method

The USACE method suggests that the pile skin friction increases linearly up to an assumed critical depth (D_c) and remains constant below that depth in cohesionless soils [43]. D_c depends on the relative density of sand and the pile diameter. Similar, but not identical, to the FHWA method, the USACE employs the α -method and bearing resistance for cohesive soils.

4.3. Revised Lambda Method

Kraft et al. [39] revised the original Lambda method after it was deemed “grossly conservative by industry” [45]. The pile penetration coefficient λ , employed by the original Lambda method for side friction in cohesive soils, was revised to account for the relative pile stiffness by proposing that λ be made a function of the term π_3 [46], which describes soil’s compressibility normalized by the pile’s compressibility. For the cohesionless soils, APILE converts the sand layers in a soil profile to equivalent clay layers and computes the side resistance using the same set of equations. Additionally, no equations for toe resistance in all soils have been proposed by the Revised Lambda method. Hence, the APILE software computes the end bearing in sands and clays using the equations proposed by the API method.

4.4. American Petroleum Institute (API) Method

Obtaining the soil properties for the design of offshore platforms can be difficult. This was the motivation behind developing the API RP2A [40], which depends on visual description of soils. For cohesive soils, the API method uses the α -method for side resistance similar to the FHWA and USACE methods, but uses its own set of equations to calculate the adhesion between the piles sides and the surrounding soil based on the ratio of undrained shear strength (s_u) to effective overburden stress. For cohesionless soil, the API method uses a table that presents friction angles and skin friction limits to aid in computing the skin friction based on the sand classification (gravel, sand, silt), and the relative density of the soil. The table also provides end bearing limits and a bearing capacity factor, N_q , for computing the end bearing.

5. Analysis

ENSOFT’s APILE Offshore 2019 software [42] was utilized for all capacity computations. APILE was selected because: (1) the design methods are pre-programmed; and (2) it is widely used among practicing geotechnical engineers. Some design methods, employ plugging assumptions inherent to their formulation. Nevertheless, APILE calculations were carried out assuming the three aforementioned plugging conditions. The authors decided to use the pre-programmed design methods in APILE to: (1) help ensure that the results are easily adopted in practice, (2) comply with the current practice; and (3) avoid claims of possible computational errors by the authors.

The authors also used python scripts to: (1) automatically generate input files for the analysis from the database; (2) extract results from APILE output files; and (3) combine the results in a single spreadsheet. This was done to automate the analysis process and speed up the calculation process.

Interpreted (measured) capacities (Q_m) were obtained from the load-settlement curves using the NYU interpretation criterion [47,48], where the capacity is that corresponding to the smallest of the following settlements: (1) the load corresponding to a settlement equal to the elastic shortening of the pile ($\frac{PL}{AE}$) plus 0.75 inches (20 mm) per the 2014 New York City Building Code; (2) 5% of the pile diameter; or (3) settlement corresponding to

first incidence of plunging or strain-softening resulting in loss of more than 5% of capacity. Calculated and computed capacities are summarized for the 74 piles in Appendix C.

5.1. Performance of Design Methods

All capacities presented in this study are unfactored (i.e., Characteristic) capacities. Calculated capacities (Q_c) using the four chosen design methods were plotted versus the interpreted capacities (Q_m) obtained from the NYU criterion for all possible plugging conditions in Figure 2. The 1:1, 1:2, and 1:0.5 lines were also plotted to underline the ideal relation between Q_c and Q_m and its boundaries. The 1:1 line represents an ideal scenario where Q_c is equal to Q_m , while the 1:2 line and the 1:0.5 line indicate over or underestimation by a factor of 2, respectively. Additionally, key statistics are listed for each design method, such as the mean, standard deviation, and the coefficient of determination (R^2). The mean and standard deviation are the descriptive statistics describing the data distribution with the mean representing the central value, and the standard deviation representing the variation in the data. R^2 is used to describe how well the fitted line, the 1:1 line, in this case, captures the behavior of the real data. Note that R^2 can have a negative value when the model selected does not follow the trend of the data. This can be clearly noticed in Figures 2 and 3 for the FHWA design method in the unplugged condition, where it is clear that the 1:1 line (chosen model) does not follow the trend of the data (red dots).

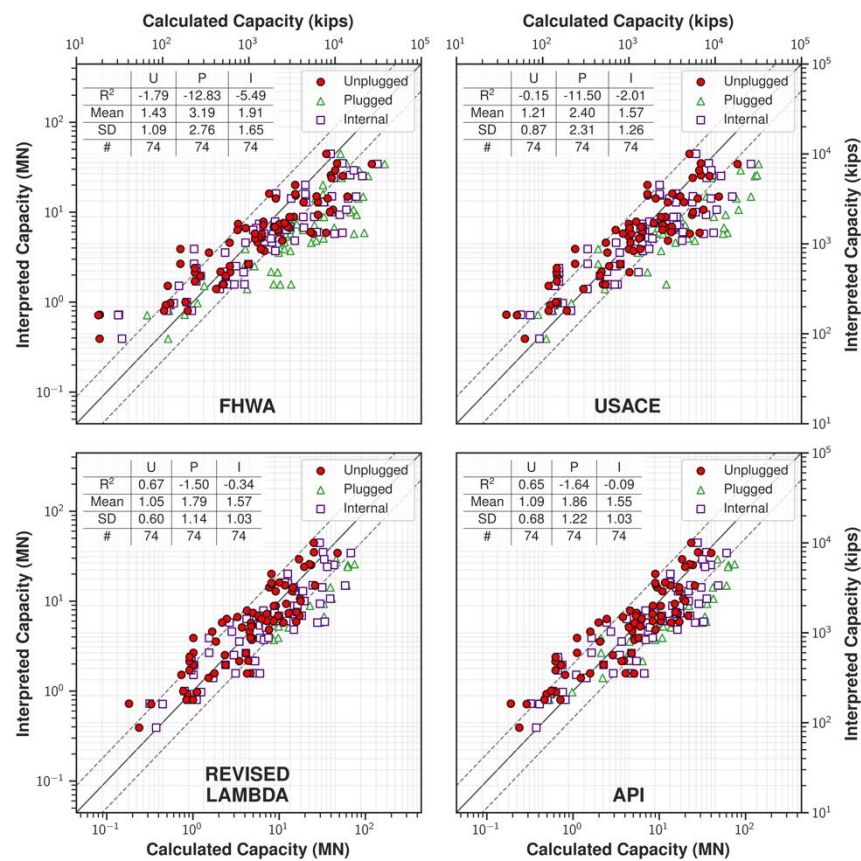


Figure 2. Calculated (Q_c) vs. interpreted (aka measured, Q_m) capacities for all plugging conditions for each design method. Statics of Q_c/Q_m are shown in the inset tables.

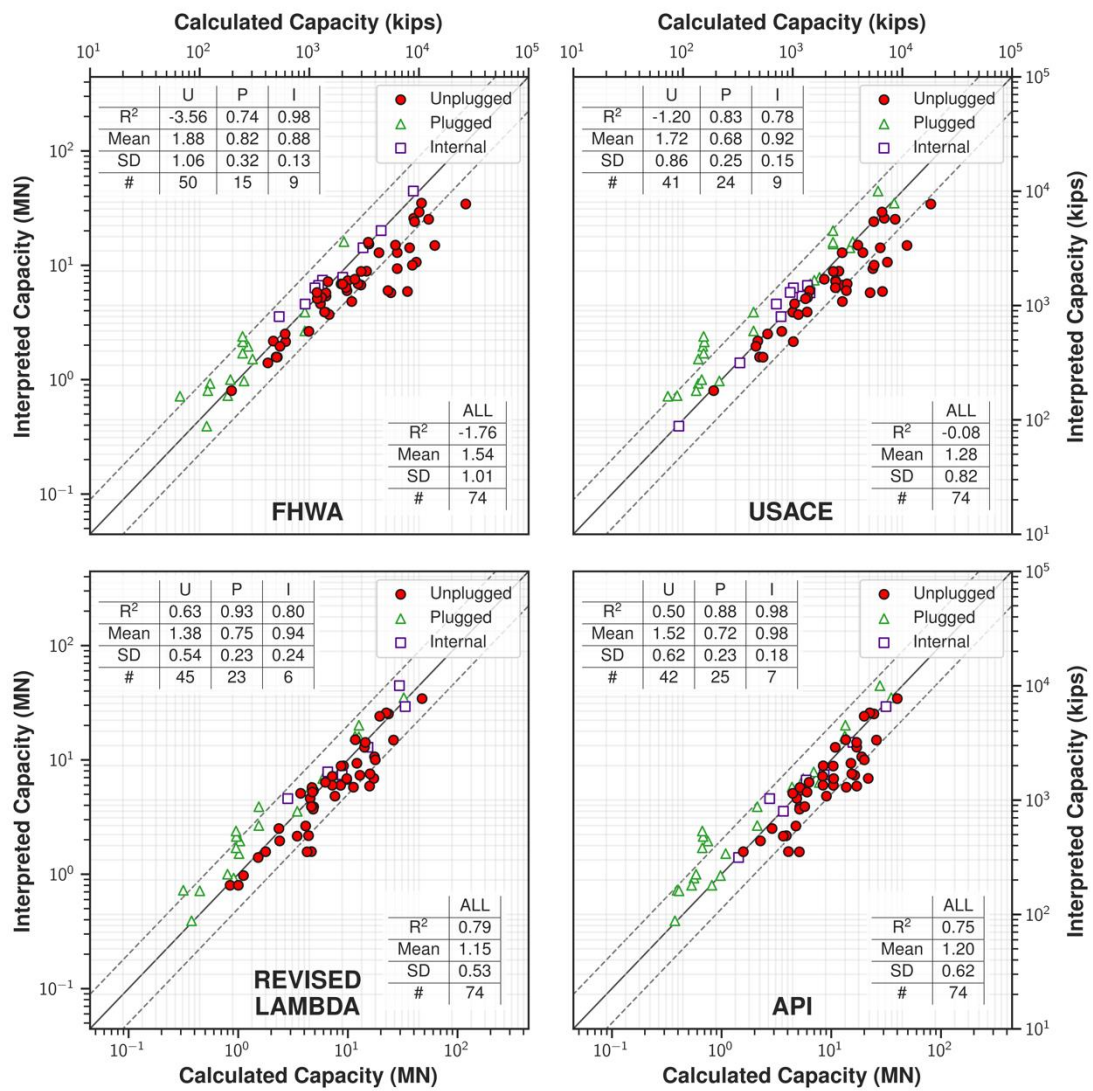


Figure 3. Calculated (Q_c) vs. interpreted (aka measured, Q_m) capacities for the best plugging conditions for each design method. Statics of Q_c/Q_m are shown in the inset tables.

A uniform datum of comparison between the performance of the various methods was established by normalizing the calculated capacities by the interpreted capacities (Q_c/Q_m), for each test, which also helps to better visualize the target value of 1. Values higher than 1 indicate that the design method is over-estimating the pile capacity, while values less than 1 indicate that the design method is conservative in its capacity estimation.

5.2. Identification of Plugging Based on Q_c/Q_m

The best-calculated capacity and the associated plugging condition were determined using each design method for each pile individually. This was determined based on the performance of Q_c/Q_m and how close is the value to the ideal value of 1. For example, for a certain pile, if the Q_c/Q_m values for a design method for the unplugged, plugged, and internal plug conditions were 1.10, 1.85, and 1.47, respectively, it was assumed that this pile was unplugged since 1.10 is closest to the ideal value of 1.00.

The measured capacity (Q_m) was plotted versus the best-calculated capacity (Q_c) in Figure 3 along with the identified plugging condition which helps identify the overall performance of all design methods and their average. It is noteworthy that the data showed significant scatter with a standard deviation ranging between 0.53 and 1.01. The scatter is attributed to a combination of factors including (1) significant variation in the calculated

capacities using the different plugging conditions and design methods, (2) quality of the geotechnical data, (3) differences in the procedures employed to conduct the static load tests; and (4) absence of information related to pile setup. Nevertheless, Figure 3 was considered as the reference for comparing any guidance resulting from this analysis, since it represents the best achievable performance given the available data. Once again, inset tables summarize the plugging condition as well as the overall performance of each design method are presented in Figure 3. Several observations are possible. First, the majority of cases are classified as unplugged. Second, only a few cases are classified as internal plug, with only 3–12% of cases being classified as internal plug. Finally, the data in Figure 3 exhibit less scatter than Figure 2, but that is to be expected.

The data in Figure 3 represent the capacity corresponding to the plugging condition closest to the interpreted value, for each design method. It was observed that the unplugged condition had superior performance compared to the other plugging conditions. This was further investigated and statistically proven for large diameter open-ended piles in the analysis presented by Rizk et al. [49].

Design methods did not always agree on whether a pile is plugged, unplugged, or internally plugged, so a voting system was used to identify the onset of plugging based on the majority of votes by the four design methods.

5.3. Relationship between Plugging Condition and the Pile Diameter, Length, and L/D Ratio

Paikowsky et al. [8] concluded that beyond a certain penetration depth to diameter ratio (L/D) most piles plug. Ko and Jeong [50] also determined that as the pile diameter increases, open-ended piles tend to become unplugged; however, these studies did not examine a large number of piles. Thus, the relationship between the plugging condition and piles' geometric properties namely diameter (D), length (L), and L/D ratio was explored in Figure 4, where piles are tagged by their voted overall plugging condition. It should be noted that important information needed to investigate plugging, such as the Plug Length Ratio (PLR), and the Incremental Filling Ratio (IFR) was not available in the databases. Hence, the discussion herein is limited to observed Q_c/Q_m values and their respective pile properties.

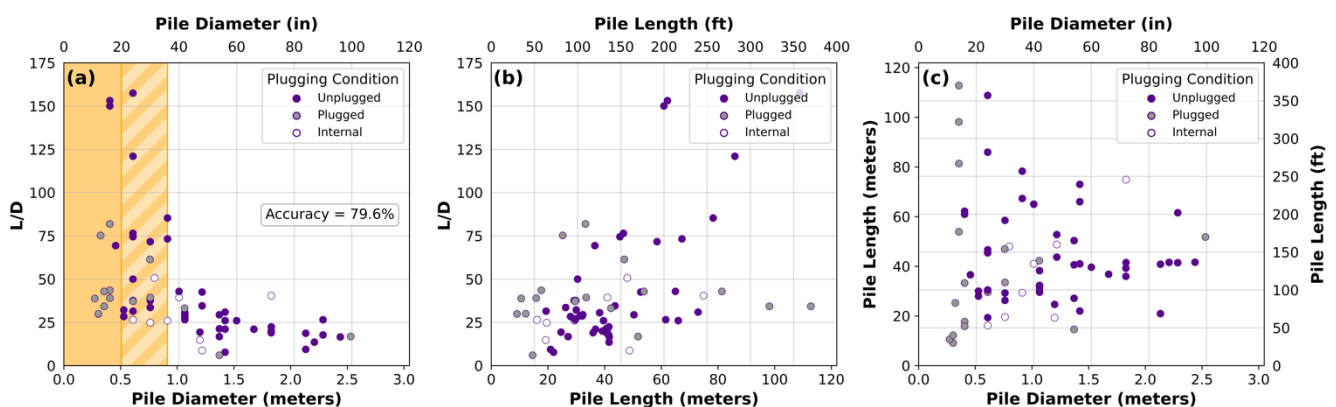


Figure 4. Relationship between: (a) L/D ratio and pile diameter, (b) L/D ratio and pile length, and (c) pile length and diameter, for the average Q_c/Q_m ratio, by the best plugging condition for each pile.

The L/D ratio was plotted against the pile diameter in Figure 4a. Multiple observations were made. It was observed that piles larger than or equal ~ 0.9 m (36 in) in diameter are likely to be unplugged (31 out of 39 cases), irrespective of L/D ratio, while piles with diameters less than 0.5 m (20 in) are likely to be plugged (12 out of 15 cases), which is expected since small diameter piles have a higher likelihood of being plugged and vice versa. This observation has critical implications for the design of large diameter open-ended piles (LDOEPs), since these are typically defined as piles larger than 36 in (~ 0.9 m) in diameter. It was also noted that the piles in between vary in terms of plugging conditions,

which suggests that this could be a transition zone between the plugged and unplugged conditions. This is shown in the figure where the shading represents the transition from a zone of plugged high likelihood, to a transition and uncertain zone, and finally a high likelihood unplugged zone. The authors also attempted to separate unplugged from internal plug, as well as internal plug from plugged; however, this was difficult due to the small number of load tests (8 cases) coded as internal plug. Using these two major zones, nearly 80% of the cases in these zones were identified correctly, which is encouraging.

The relationship between L/D and length for all piles under consideration coded by the voted plugging conditions is presented in Figure 4b. Similarly, the relationship between length and diameter is presented in Figure 4c. It was observed that the majority of the plugged piles are small diameter piles with low L/D ratios ($L/D < \sim 50$). No further pattern of plugging is discernable, as the data scatter makes it hard to make conclusive observations regarding pile plugging. In particular, the available data do not support the popular notion that most piles plug beyond a certain L/D ratio. Notably, Paikowsky et al. [8] suggest that piles with L/D smaller than 75 are unlikely to plug, but it is difficult for us to agree considering the data presented in Figure 4. In addition, prior studies suggest that when a pile plugs, load is transferred by arching to the inner pile surface within the first two pile diameters [51]; thus, it was concluded that soil, driving, and load testing conditions have significant effects on plugging of piles, and recommendations based solely on length or L/D are difficult to formulate based on the available data.

5.4. Relationship between Plugging Condition and Soil Information

The relationship between the plugging condition and soil properties was investigated next. Histograms for the voted plugging condition with respect to the predominant soil type along the pile length and the bearing soil layer are presented in Figure 5a,b, respectively. The predominant soil type was determined by taking the weighted average of the heights of the soil layers along the depth of the piles. Predominant soil types were classified into three arbitrary groups depicting sand (0–30% clay), mixed soils (30–70% clay) and clayey soils (70–100% clay). Once again, no clear inference could be drawn, except that (1) piles bearing in sand had a higher tendency to be unplugged, which could be attributed to the frictional resistance of clay, increasing the likelihood of the pile being plugged in clay; and (2) that the predominant soil type does not materially influence the analysis. This observation is somewhat surprising, and the occurrence of plugging in sand is likely related to its relative density, a factor that is not accounted for in Figure 5.

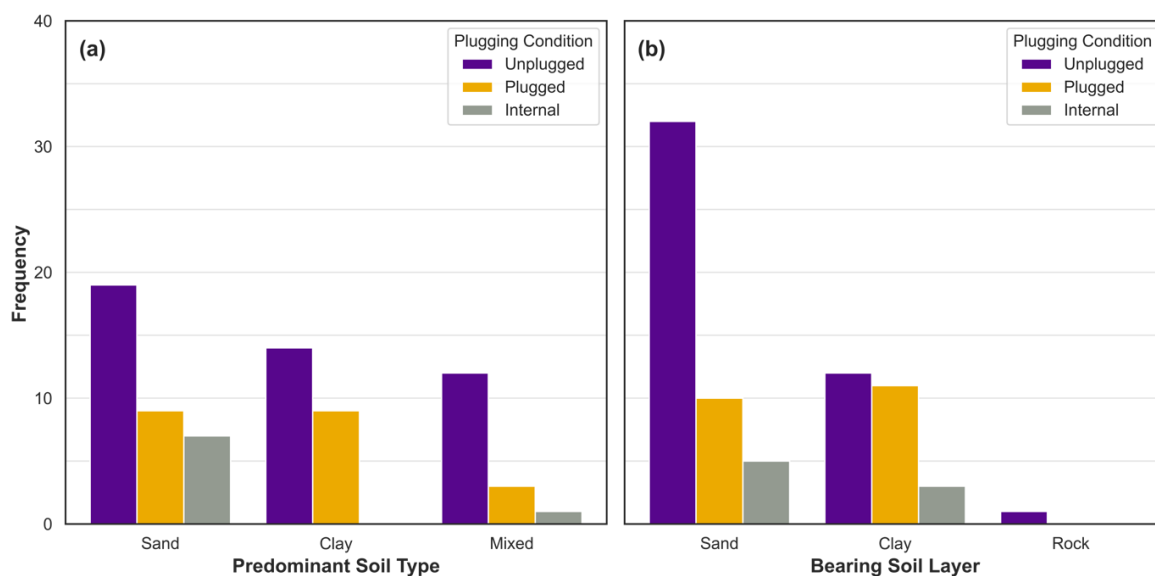


Figure 5. Histograms of (a) the predominant soil type, and (b) the bearing soil layer for each plugging condition.

6. Proposed Interaction Diagram for Plugging

6.1. Development of Interaction Diagram

The authors explored if plugging could be better forecasted using an interaction diagram that separates piles into two zones (plugged and unplugged) based on both the values of the pile diameter and the L/D ratio. Multiple interaction diagrams with $D = 0.5\text{--}1.78\text{ m}$ (20–70 in) and $L/D = 75\text{--}125$ were explored (121 interaction diagrams in total), and their performance was evaluated by computing the number of cases correctly forecasted based on the voted overall plugging condition. The authors also explored the use of two lines to separate the cases into three zones representing plugged, internally plugged, and unplugged; however, the accuracy was lower than using a single line separating the plugged from unplugged conditions. This could be attributed to the small number of internally plugged cases.

The highest achieved forecasting accuracy using an interaction diagram was 74.3% (55 out of 74 cases forecasted correctly) and was achieved by five possible lines. These five lines are plotted in Figure 6a where the shaded zone is where the piles are likely to be plugged. The initial proposal was to find the line with the highest accuracy and use it; however, upon finding 5 lines achieving identical accuracies, it was theorized that the area created by the union of these 5 lines would give more confidence in the likelihood of the plugging occurrence. This union zone is presented in Figure 6b along with the associated accuracy.

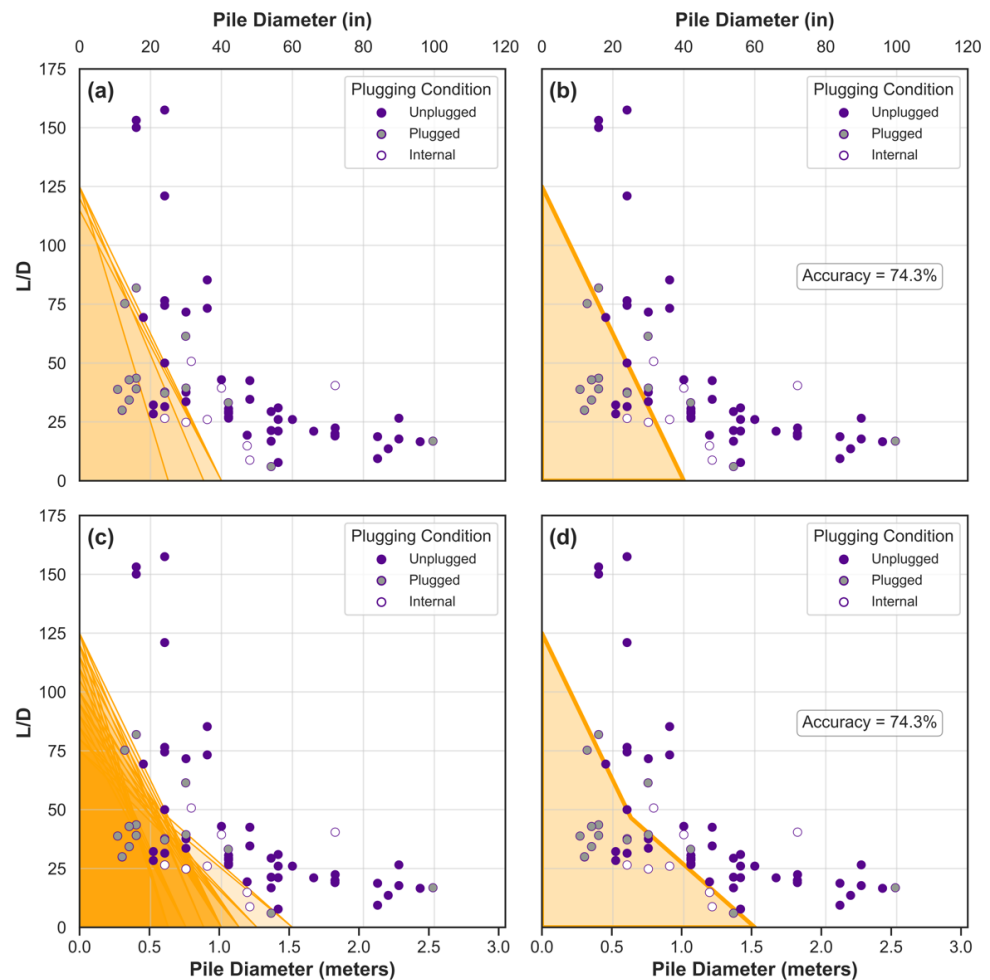


Figure 6. Performance of various interaction diagrams for forecasting pile plugging based on pile dimensions. (a) The top performing 5 interaction diagrams; (b) The union zone created by the top 5 interactive diagrams and their respective accuracy; (c) The top achieving 25 interaction diagrams; (d) The union zone created by the top 25 interactive diagrams and their respective accuracy.

The second highest accuracy was 73% (54 out of 74) and was achieved by 20 possible lines. All 25 lines are plotted in Figure 6c, where the shaded zone is where the piles are likely to be plugged. Again, upon finding 25 lines achieving nearly identical accuracies, it was theorized that the area created by the union of these 25 lines would give more confidence in the likelihood of the plugging occurrence. This union zone is presented in Figure 6d along with the associated accuracy.

6.2. Diameter Criterion

Using both interaction diagrams resulted in the same accuracy of 74.3%, which means that the plugging condition of the pile could be forecasted approximately 3 out of 4 times. This occurs because no interaction diagram was able to increase the rate of positive identification of plugging while reducing the rate of false identification. A much larger dataset is likely needed to overcome this challenge. At any rate, interaction diagrams do not represent an improvement over using the straightforward diameter criterion (Figure 4a). Hence, the authors chose the original diameter criterion proposed in Figure 4a for a couple of reasons. First, the diameter criterion is a more discreet and intuitive concept, and easier to comprehend. Second, the diameter criterion resulted in a higher accuracy, rendering the Diameter–L/D interaction diagram inferior to the diameter criterion.

6.3. Testing of the Diameter Criterion & Interaction Diagram

DFLTD contained 23 tests where CPT data were available [Appendices A and B]. These load tests were initially excluded from the analysis because they lacked the SPT data required for computing the capacity using the FHWA, USACE, Revised Lambda, and API design methods. Therefore, the author used these 23 cases to test the diameter criterion (Figure 4) and the interaction diagrams (Figure 6). A similar methodology and voting routine were used and APILE was again utilized. Four CPT design methods were employed namely: (i) the Norwegian Geotechnical Institute (NGI) method [52,53]; (ii) the Imperial College Pile (ICP) method [54]; (iii) the Fugro method [55]; and (iv) the University of Western Australia (UWA) method [56]. It is essential to acknowledge that, while APILE employs FUGRO-04 and UWA-05, updated methods (FUGRO-10, and UWA-13) have since been developed. Some design methods employ plugging assumptions inherent to their formulation. Nevertheless, APILE calculations were carried out assuming the three aforementioned plugging conditions [Appendix D]. The authors decided to use the pre-programmed design methods in APILE to: (1) help ensure that the results are easily adopted in practice, (2) comply with the current practice; and (3) avoid claims of possible computational errors by the authors.

The capacities corresponding to the three plugging conditions and their statistics for the four CPT methods are presented in Figure 7. On average, the performance statistics in terms of average Q_c/Q_m and its standard deviation (Target 1 and 0) is somewhat better than the classic methods presented earlier (Figure 3), but scatter between measured and calculated capacities persists.

The relationship between L/D and diameter for all CPT tests is presented in Figure 8, with the presumed plugging condition obtained via voting identified using the symbols U for unplugged, P for plugged. The diameter criterion and the two previously identified interaction diagrams are also superimposed on the data. One difference is that the CPT methods can in fact identify internal plugged cases and two piles were identified as internally plugged. These two cases are shown in the figures, designated by the letter I, but excluded when computing accuracy. The accuracy of the diameter criterion was found to be 60% while the accuracy of the two interaction diagrams was found to be 60.9% and 56.5%. These results suggest that the diameter criterion offers results that are as good as the interaction diagrams. More importantly, it suggests that the accuracy of the diameter criterion is in the order of $70 \pm 10\%$.

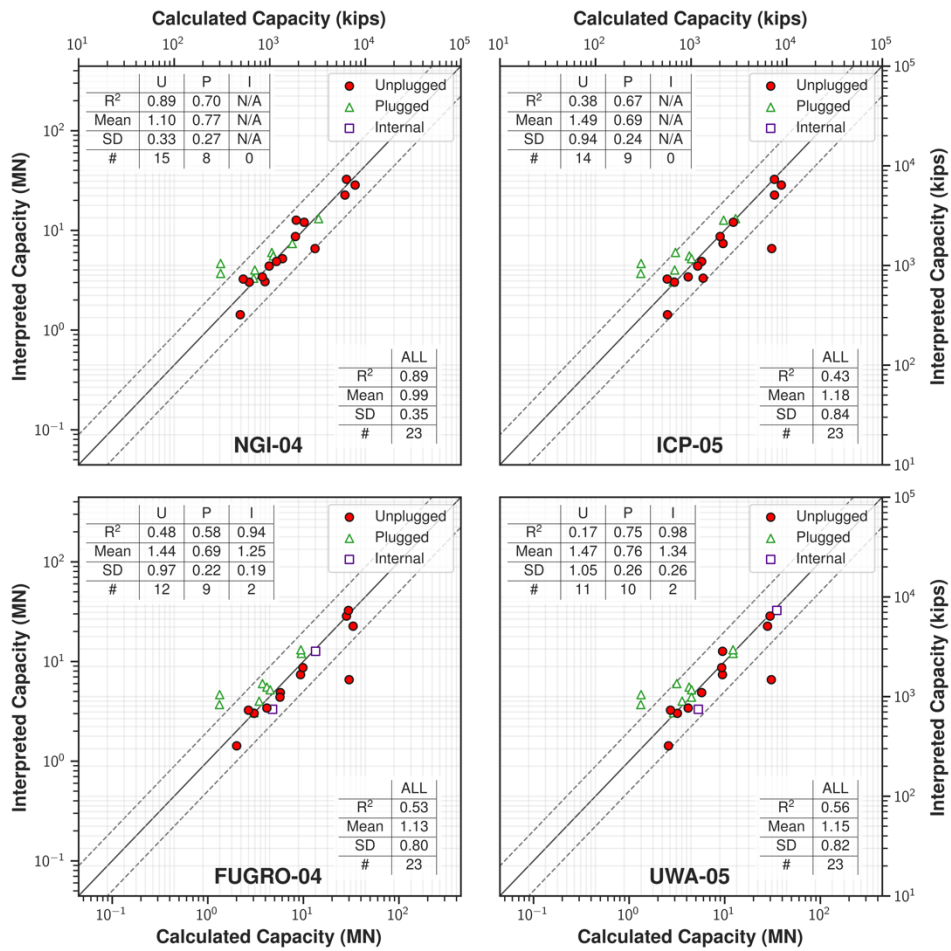


Figure 7. Calculated (Q_c) vs. interpreted (aka measured, Q_m) capacities for the best plugging conditions for the CPT design methods. Statics of Q_c/Q_m are shown in the inset tables.

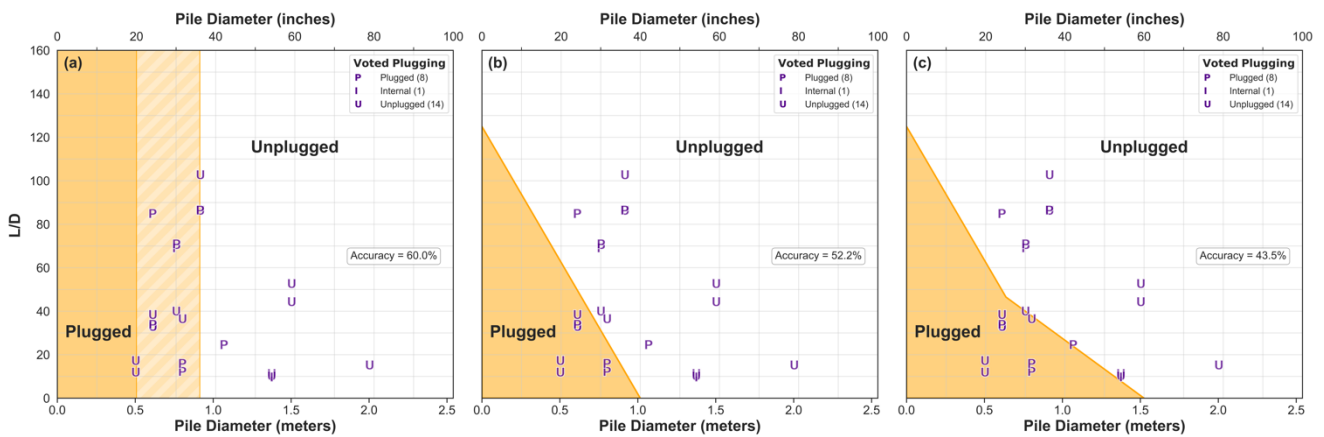


Figure 8. Testing the performance of the diameter criterion and two interaction diagrams using a dataset of CPT piles (a) The proposed diameter criterion and its respective accuracy; (b) The proposed interaction diagram created by the union of the top 5 interactive diagrams and its respective accuracy; (c) The proposed interaction diagram created by the union of the top 25 interactive diagrams and its respective accuracy.

7. Validation of the Proposed Diameter Criterion

The performance of the diameter only criterion was validated using 24 published load tests where in-situ plugging performance was reported. None of these piles were

employed previously in our analyses, so this represents a true arm’s length check on the proposed criterion. The new piles in the test dataset ranged in diameter from 0.33 to 1.58 m (13–62 inches), and in length from 9 to 86 m, (30–282 ft). All chosen piles included information about either the Incremental Filling Ratio (IFR), or the Plug Length Ratio (PLR). An IFR of 1.00 indicates that the pile is completely unplugged, while an IFR of 0 represents a completely plugged pile, and anything in between implies a partially plugged pile. Since the measured IFR values are not always 0 s and 1 s, and since the proposed interaction diagram does not account for the partially plugged condition, it was decided that an unplugged pile is any pile with an IFR > 0.3, and a plugged pile is any pile with an IFR < 0.3. The authors performed sensitivity analyses and the results of the analyses remained consistent when the plugging threshold was set to IFR in the range of 0.2 to 0.6.

The test piles are summarized in Table 1 and are plotted in Figure 9, with the actual plugging condition identified using the symbols U for unplugged, P for plugged. The actual plugging condition based on the recorded IFR value, along with the forecasted plugging condition based on the diameter criterion are also shown in Table 1. The proposed diameter criterion successfully forecasted the plugging condition in 10 cases out of the 14 test cases that plot in the plugged and the unplugged zones with an accuracy of 71% and was off in 4 cases. The remaining 10 cases are scattered in the transition zone, and hence the plugging condition cannot be determined with confidence since the likelihood of being plugged and unplugged are equal.

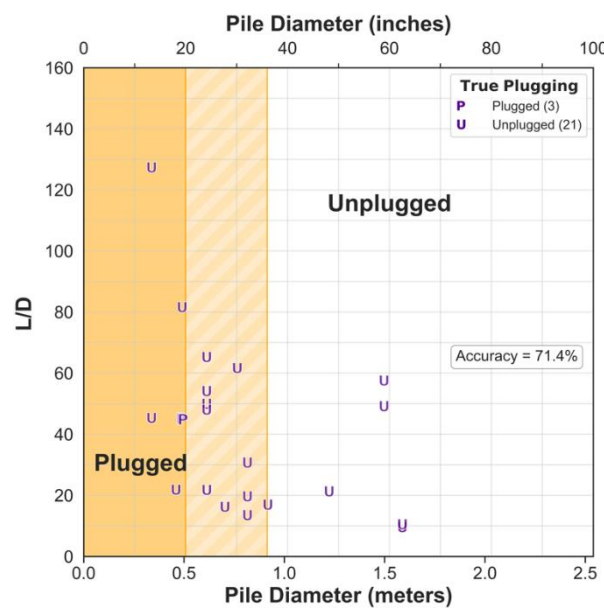


Figure 9. Test Piles used to evaluate the performance of the proposed diameter criterion, showing the actual plugging condition and the resulting accuracy.

These observations, confirm that the proposed diameter criterion can be employed for preliminary determination of plugging, factoring in that its accuracy is on the order of 70%; however, the results are somewhat skewed by only 3 out of 24 tests in the validation data set exhibiting in-situ plugging.

Table 1. Test Piles used to evaluate the performance of the proposed interaction diagram, and the actual and forecasted plugging condition.

#	Reference	Pile ID	Diameter m (in)	Length m (ft)	L/D	IFR (%)	Plugging Condition	
							Actual	Forecasted
1	Jeong and Ko [23]	TP-2	0.7 (27.6)	11.4 (37.4)	16.3	60.0	Unplugged	N/A
2		TP-3	0.9 (36)	15.5 (50.9)	17.0	60.0	Unplugged	Unplugged

Table 1. Cont.

#	Reference	Pile ID	Diameter m (in)	Length m (ft)	L/D	IFR (%)	Plugging Condition	
							Actual	Forecasted
3	Jardine et al. [54]	-	0.8 (30)	47 (154.2)	61.7	89.0	Unplugged	N/A
4	Kikuchi [57]	TP4	1.5 (58.8)	73.5 (241.1)	49.2	100.0	Unplugged	Unplugged
5		TP5	1.5 (58.8)	86 (282.2)	57.6	100.0	Unplugged	Unplugged
6	De Nicola and Randolph [24]	LOD1	1.6 (62.4)	15.7 (51.5)	9.9	65.0	Unplugged	Unplugged
7		MOD1	1.6 (62.4)	15.2 (49.9)	9.6	85.0	Unplugged	Unplugged
8		DOD2	1.6 (62.4)	16.7 (54.8)	10.5	115.0	Unplugged	Unplugged
9	Han et al. [58]	-	0.6 (24)	30.5 (100)	50.0	70.0	Unplugged	N/A
10	Liu et al. [59]	P1	0.5 (19.2)	22 (72.2)	45.1	0.0	Plugged	Plugged
11		P2	0.5 (19.2)	22 (72.2)	45.1	0.0	Plugged	Plugged
12		P3	0.5 (19.2)	22 (72.2)	45.1	0.0	Plugged	Plugged
13	Olson and Shantz [29]	Bent E31R	0.6 (24)	13.3 (43.6)	21.8	83.0	Unplugged	N/A
14	Tveldt et al. [60]	16	0.8 (32.0)	11 (36.1)	13.5	88.0	Unplugged	N/A
15		25	0.8 (32.0)	16 (52.5)	19.7	88.0	Unplugged	N/A
16		25	0.8 (32.0)	25 (82.0)	30.8	88.0	Unplugged	N/A
17	Jardine and Standing [61]	C1	0.5 (18.0)	10 (32.8)	21.9	78.0	Unplugged	Plugged
18	Williams et al. [62]	P	1.2 (48.0)	26 (85.3)	21.3	95.0	Unplugged	Unplugged
19	Yang et al. [63]	K24-1	0.6 (24)	33 (108.3)	54.2	74.0	Unplugged	N/A
20		K24-2	0.6 (24)	39.8 (130.6)	65.3	74.0	Unplugged	N/A
21		K24-3	0.5 (19.2)	39.8 (130.6)	81.6	73.0	Unplugged	Plugged
22		K34-1	0.6 (24)	29.3 (96.1)	48.1	82.0	Unplugged	N/A
23	Mayne [64]	AL 1	0.3 (13.2)	15.2 (49.9)	45.4	71.0	Unplugged	Plugged
24		AL 2	0.3 (13.2)	42.7 (140.1)	127.4	71.0	Unplugged	Plugged

8. Practical Significance of Results

The data presented in this study suggest that forecasting the plugging of pipe piles based solely on pile dimensions and the geotechnical profile is difficult. This is not surprising considering that plugging is influenced by a myriad of installation effects that are not captured by many of the design methods in common use. Nevertheless, forecasting the plugging before driving is necessary not only to correctly compute the capacity, but also to ensure drivability to the desired depth, especially for cases of non-uniform pile wall thickness.

The presented results have two implications. The first is that large diameter piles, piles with diameters larger than ~0.9 m (36 inches), are highly likely to be unplugged. The second is that piles smaller than 0.5 m (20 inches) are likely to be plugged. The design engineer has two options. The first is to assume that all piles are unplugged. This approach is in our opinion best when estimation of the correct ultimate capacity is desirable. Our opinion is based on the mean normalized capacity being closest to 1 for the unplugged assumption when considering the 74 cases examined in Figure 2 using the 4 design methods. This opinion is also supported by examining the capacities computed in Appendix D using the CPT design methods. Alternatively, the proposed diameter criterion can be used to forecast the onset of plugging when determination of plugging is paramount, for example to size the driving equipment. Utilization of the proposed diameter criterion should however be limited to piles in the same size ranges considered here in ($L > 9$ m (30 ft), $D = 0.25$ – 2.5 m (10–100 inches), and $L/D = 6$ – 150).

9. Limitations

Several limitations were encountered in this study. The first was the lack of plugging information such as the soil column depth inside the piles, or the Incremental Filling

Ratio (IFR). This information is necessary to positively identify the onset of plugging in pipe piles. Because nearly all the piles were not instrumented, the authors are unable to separate the effects of plugging on base and shaft resistance. In addition, the authors are unable to discern when plugging occurred. Some piles may have driven as coring, and plugged during load testing (Static Plugging), while others may have plugged during driving (Dynamic Plugging). Similarly, partial/intermittent plugging is not considered; the analysis presumes a PLR of 1 or 0, while field data generally suggest PLRs between 0.5 and 1 [3]. Finally, plugging may also influence both stiffness and load transfer, but the nature of the analysis precludes identifying these effects. Consequently, that limited the analysis to being a statistical evaluation based on the pile properties and the observed measured and computed capacities only.

A second limitation was that only a few piles (8 cases) were identified as developing an internal plugging condition, leading to the decision to marginalize the internal plugging condition in the process of developing the proposed diameter criterion and in the analysis overall.

The third limitation was the lack of information about the age of testing for some cases in the employed dataset. Age of testing affects pile capacity significantly, which is also associated with the actual plugging condition. Hence, the authors opted for employing the pile geometric properties. Finally, the quality of the available data is not always excellent, and in many cases lacks vital information regarding either the driving system or the soil conditions.

Finally, on average the performance of the design methods used to deduce the plugging condition has been less than optimal (Table 2). All methods appear to consistently overestimate the capacity of unplugged piles and underestimate the capacity of plugged and internally plugged piles (Figures 3 and 7). Many individual cases are overestimated or underestimated by a factor of two. Some design methods overestimate the capacity by nearly 90% under certain conditions (e.g., FHWA Unplugged in Figure 3). These shortcomings stem from design methods having well-recognized limitations which are beyond the scope of this work. Therefore, the authors refrained from offering any design method-specific recommendations and opted for general recommendations based on the voted plugging condition.

Table 2. Average performance statistics of all design methods employed in this study.

Method	Average Q_c/Q_m	Std. Dev. Q_c/Q_m
FHWA	1.54	1.01
USACE	1.28	0.82
Revised Lambda	1.15	0.53
API	1.2	0.62
NGI-04	0.99	0.35
ICP-05	1.18	0.84
FUGRO-04	1.13	0.80
UWA-05	1.15	0.82

10. Conclusions

The propensity for plugging based on basic pile properties such as pile diameter, length, and L/D ratio was investigated using a database of load tests on 74 open-ended pipe piles. The closeness between the capacity interpreted from a load test and that computed for three plugging conditions was used to identify plugging for each design method, then a voting system was employed to decide the overall plugging condition of a pile. Four commonly used designed methods were used to compute the calculated capacity including: (1) FHWA, (2) USACE, (3) Revised Lambda, and (4) API. The results

were checked using 23 load tests where CPT soundings were available and a similar voting methodology was employed but using four CPT-based pile design methods including (i) NGI-04, (ii) UWA-05, (iii) FUGRO-04 and (iv) UWA-05 methods. Finally, the results were validated using 24 case histories where plugging records have been reported. A summary of the findings is presented below:

Most of the piles in the database of 74 piles used in this study appear to be unplugged, evidenced by that condition providing the closest capacity to the one interpreted from the load test. This was also the case for the test dataset of 24 case histories where plugging records have been reported;

No plugging pattern was found based on a diameter-length relationship or a length-L/D ratio relationship, or soil condition, as data was largely scattered;

Piles larger than 0.9 m (36 inches) in diameter have higher likelihood of being unplugged, while piles smaller than 0.5 m (20 inches) tend to be plugged. These dimensions are proposed as a diameter criterion for preliminary determination of the plugging condition of a pile with an average accuracy of $70 \pm 10\%$.

Author Contributions: Both authors contributed to the study conception and design. The specific roles are: data manipulation, software development, investigation, formal analysis, methodology, visualization, writing original draft, A.K.; conceptualization, supervision, validation, project administration, writing review and editing, M.I. All authors have read and agreed to the published version of the manuscript.

Funding: This research received no external funding.

Institutional Review Board Statement: Not applicable.

Informed Consent Statement: Not applicable.

Data Availability Statement: All data used during the study appears in the submitted article.

Acknowledgments: This study employed data from FHWA DFLTD v2 as well as Roy Olson piling database. The authors are grateful to Roy Olson and FHWA for providing the data. The databases were ported from their original sources to a relational database by Nick Machairas, now Data and Analytics Leader at Haley and Aldrich, as part of his doctoral dissertation at NYU. Drew Rizk, PE, now Associate Principal/Vice President GZA Geoenvironmental, reviewed the geotechnical data of all load tests as part of his master's thesis at NYU. The authors gratefully acknowledge these previous efforts, without which this work would not have been possible.

Conflicts of Interest: The authors declare no conflict of interest and certify that they have no affiliations with or involvement in any entity with any financial, or non-financial, interest in the subject matter or materials discussed in this manuscript.

Appendix A. Open-Ended Pipe Piles Adopted into This Study from the FHWA DFLTD v.2 Database

ID	Project ID	Project	Material	Pile ID	Load Test ID	OD (in)	ID (in)	L (ft)	CPT Data	Soil Profile ID	Major Soil Type	Ref.
N-1	234	Salinas River Bridge, USA	S	1	1	60	59	130	No	B-5	Sand	
N-2	843	108 GRL Piles-3rd Lake Wash. BR, WA, USA	S	1	1	48	46	160	No	GRL Piles #108	Sand	[26]
N-3	1001	Port Mann Bridge, Canada	S	5	1	72	70	246	No	DFSL	Mixed	[65]
N-4	1002	Red Sea Coast, Saudi Arabia	S	1	1	56	54	240	No	Boring-A	Sand	[66]
N-5				2	1	56	54	217	No			
N-6				4	1	56	54	135	No	Boring-B	Sand	
N-7				5	1	56	54	72	No			
N-8	1003	Louisiana Highway 1 Improvements Phase 1B, USA	S	1	1	30	29	195	Yes	1	Clay	[67]
N-9	1004	Tokyo Port Bay Bridge, Japan	S	1	1	59	57	261	Yes	Generalized	Mixed	[57]
N-10				2	1	59	57	302	Yes			
N-11	1005	Salinas River Bridge, USA	S	1	1	72	71	118	No	UTB-44	Mixed	[68]
N-12	1006	I-880 Port of Oakland Connector Viaduct, USA	S	1	1	42	41	88	Yes	1	Clay	
N-13	1007	I-880 Oakland Bridge Replacement, USA	S	1	1	42	41	106	No	Generalized Boring	Clay	[26]
N-14				2	1	42	41	106	No			
N-15	1008	Santa Clara River Bridge, USA	S	1	1	84	81	69	No	00-2	Mixed	[68]
N-16				2	1	84	81	134	No			
N-17	1009	Noto Peninsula New Highway Route Bridges, Japan	S	1	1	31	31	36	Yes	DFSL	Clay	[69]
N-18				2	1	31	31	36	Yes			

ID	Project ID	Project	Material	Pile ID	Load Test ID	OD (in)	ID (in)	L (ft)	CPT Data	Soil Profile ID	Major Soil Type	Ref.
N-19	1010	Pentre Site, Great Britain	S	1	1	30	28	192	No	101	Clay	[70]
N-20	1011	Woodrow Wilson Bridge over Potomac River, VA and MD, USA	S	1	1	54	52	165	No	ID-63	Mixed	[68]
N-21				2	1	42	40	126	No	ID-64	Mixed	
N-22				3	1	36	34	96	No	ID-65	Sand	
N-23	1012	Jin Mao Building, China	S	1	1	36	34	262	Partial	Generalized Boring	Mixed	[71]
N-24				2	1	36	34	262	Partial			
N-25	1013	Hokkaido, Japan	S	1	1	40	38	135	No	Generalized Boring	Sand	[26]
N-26	1014	Chiba, Japan	S	1	1	31	30	157	No	Generalized Boring	Sand	[72]
N-27	1019	EURIPIDES Joint Industry Project-Offshore test piles, Netherlands	S	1	1	30	27	101	Yes	CPT-36	Sand	[26]
N-28				3	1	30	27	154	No			
N-29				4	1	30	27	154	No			
N-30				4	2	30	27	154	No			
N-31	1020	Sakonnet River Bridge (Route 138), USA	S	1	1	72	69	136	No	Generalized Boring	Sand	[73]
N-32	1021	Annacis Throughway Bridge Project-Highway 91, Canada	S	1	1	36	35	221	No	Generalized CPT	Clay	[74]
N-33				2	1	36	35	257	No			
N-34				3	1	36	35	309	Yes			
N-35	1023	Berenda Slough Bridge, USA	S	1	1	42	41	106	No	98-5	Sand	[68]
N-36	1024	Gulf Intracoastal Waterway West Closure Complex Test Site 3	S	2	1	30	29	190	Partial	ALGSGS-08-2U	Clay	[75]
N-37	1025	I-880 5th Street Overhead Bridge, USA	S	1	1	96	93	137	No	Generalized Boring	Clay	[76]

ID	Project ID	Project	Material	Pile ID	Load Test ID	OD (in)	ID (in)	L (ft)	CPT Data	Soil Profile ID	Major Soil Type	Ref.
N-38	1035	Highway 32 Stony Creek Bridge (No. 11-0029), USA	S	1	1	100	96	170	No	00-6	Mixed	[77]
N-39	1055	Feather River Bridge (Caltrans Bridge No. 18-0009), USA	S	1	1	48	46	173	No	1	Sand	[78]
N-40	1056	Mad River Bridge (Caltrans Bridge No. 04-0025L), USA	S	1	1	87	84	136	No	1	Sand	[79]
N-41	1057	Russian River Bridge, USA	S	1	1	66	64	121	No	1	Sand	[80,81]
N-42	1060		S	1	1	48	46	143	No	1	Sand	
N-43	1061	Feather River Bridge, USA	S	1	1	90	87	136	No	1	Sand	[26]
N-44	1061		S	2	1	90	87	202	No			
N-45	1062	Santa Clara River Bridge, USA	S	1	1	72	69	129	No	1	Sand	[82]
N-46				1	1	42	41	98	No	1	Mixed	
N-47	1063	Port of Oakland, USA	S	2	1	42	41	103	No	2	Clay	[83]
N-48				3	1	42	41	97	No	3	Mixed	
N-49	1068	Port of Toamasina Offshore Jetty	S	2	1	40	38	213	No	NP-04	Sand	[84]
N-50	1069	Trans-Tokyo Bay Highway, Japan	S	1	1	79	76	203	Partial	DFSL	Sand	[85]
N-51		Legislative Route 795 section B-6 Philadelphia, Pennsylvania, USA	S	1	1	30	29	96	No	PLT-E	Mixed	
N-52	1070			2	1	30	29	64	No	PLT-C	Sand	[86]
N-53				3	1	30	29	86	No	B-620	Mixed	
N-54	1071	Nippon Steel Blast Furnace Foundations, Japan	S	2	1	47	46	81	No	DFSL	Sand	[87]
N-55				3	1	47	46	63	No			

ID	Project ID	Project	Material	Pile ID	Load Test ID	OD (in)	ID (in)	L (ft)	CPT Data	Soil Profile ID	Major Soil Type	Ref.
N-56	1072	Tilbrook Grange Site, Great Britain	S	1	1	30	27	110	No	201	Clay	[70]
N-57	1102	I-664 Bridge, USA	C	1	1	54	44	48	No	B-66	Sand	[68]
N-58				7	1	54	44	133	No	B-71	Sand	
N-59	1103	San Mateo-Hayward Bridge, USA	C	1	1	42	28	139	No	DFSL-1	Clay	[68]
N-60	1104	St. George Island Bridge Replacement. Pier 20 (Test Pile LT-1), USA	C	1	4	54	38	80	Partial	B-20	Sand	[69]
N-61	1105	US 13 Chesapeake Bay Bridge—Tunnel, USA	C	6	1	54	42	96	Partial	DFSL-6	Mixed	[68]
N-62	1106	Crossbay Blvd. Bridge Over North Channel, USA	C	1	1	54	44	89	No	DFSL	Sand	[88]
N-63	1116	St. George Island Bridge Replacement. Pier 124 (Test Pile LT-5), USA	C	1	2	54	38	80	Partial	1	Sand	[68]
N-64	PHC-2	Wuhu Bridge, China	C	-	-	31.5	21	96	Yes	K27	Sand	[82]
N-65	10	Seismic Retrofit Program-Hwy 280, USA	S	14	2	16	15	109	No	B2	Mixed	[26]
N-66	10		S	28	1	13	12	83	No	B8	Mixed	
N-67	10		S	29	2	16	15	204	No	B2	Mixed	
N-68	10		S	30	1	16	15	200	No	B2	Mixed	
N-69	124	Ventura Underpass Br # 52-178, USA	S	69	1	12	11.7	30	No	B-1A	Sand	[26]
N-70	129	Nyeland Acres O.C Sta103+00, USA	S	24	1	11	10.5	35	No	B-2	Sand	[26]
N-71	228	Bayshore Fwy Viaduct Site C, USA	S	1	1	16	15	58	No	B-5	Sand	[26]
N-72	228		S	2	1	16	15	52	No	B-5	Sand	

ID	Project ID	Project	Material	Pile ID	Load Test ID	OD (in)	ID (in)	L (ft)	CPT Data	Soil Profile ID	Major Soil Type	Ref.
N-73	229	Bayshore Fwy Viaduct Site B, USA	S	2	1	24	23	64	No	B-4	Clay	[26]
N-74	230	Bayshore Fwy Viaduct Site D, USA	S	2	1	24	23	53	No	95-2	Sand	[26]
N-75	231	Bayshore Fwy Viaduct Site E, USA	S	1	1	24	23	98	No	95-3	Clay	[26]
N-76	231	USA	S	2	1	24	23	97	No	95-3	Clay	
N-77	235	Bayshore Fwy Viaduct Site F, USA	S	1	2	24	23	73	Yes	CPT-1	Mixed	[26]
N-78	235	USA	S	2	1	24	23	72	Yes	CPT-1	Mixed	
N-79	707	ABEF Research on Foundation # 84, Great Britain	C	7	2	20	13	30	Yes	CPT1	Sand	[26]
N-80	707	Great Britain	C	8	2	20	13	25	Yes	CPT1	Sand	
N-81	788	GRL Piles-LTV Cont. Caster, Ohio, USA	S	2	1	18	17	120	No	GRL 42	Mixed	[26]
N-82	789	GRL Piles-ODOT State Rte 22, Ohio, USA	S	1	1	12	11.6	40	No	GRL 44	Sand	[26]
N-83	1024	Gulf Intracoastal Waterway West Closure Complex Test Site 3, USA	S	1	1	24	23	190	Yes	ALGSGS-08-10U	Clay	[74]

Appendix B. Open-Ended Steel Pipe Piles Adopted into This Study from the Olson's Database

ID	Olson Project ID	Project Location	OD (in)	ID (in)	L (ft)	CPT Data	Major Soil Type	Original Source
N-84	43	British Columbia, CAN	24	23	100	No	Clay	[89]
N-85	44		24	23	153	No	Clay	
N-86	68	Alsancak Harbor, Turkey	20.8	18.2	98	No	Clay	[90]
N-87	70		20.8	18.2	92	No	Clay	
N-88	487	Empire, Louisiana	14	11.4	177	No	Clay	[91]
N-89	489		14	9.75	267	No	Clay	
N-90	491		14	9.75	322	No	Clay	
N-91	493		14	9.75	370	No	Clay	
N-92	494		14	9.75	370	No	Clay	
N-93	495	Kontich, Belgium	24	22	79	Yes	Clay	[92]
N-94	497		24	22	68	Yes	Clay	
N-95	527	British Columbia, CAN	24	23	149	No	Clay	[89]
N-96	868	Eugene Island, USA	24	18.75	357	No	Clay	Unpublished Data, Source: Confidential
N-97	869		24	18.75	282	No	Clay	

Appendix C. Calculated Capacities for the SPT Design Methods

Load Test Information			Calculated Capacities (kips)											
Case ID	Nominal Resistance (kips)	Max. Applied Load (kips)	FHWA			USACE			REVISED LAMBDA			API		
			U	P	I	U	P	I	U	P	I	U	P	I
N-1	2100	2100	6338	17,831	11,352	5390	13,240	7835	2717	7384	6696	3398	8065	6476
N-2	1030	2000	599	5290	917	539	3472	711	376	1712	636	356	1692	617
N-3	10,022	12,061	7937	11,594	8901	5037	6001	6001	5679	6643	6643	5272	6236	6236
N-4	1328	1417	7855	21,809	12,204	6587	13,864	9612	3550	7598	7598	3835	7884	7348
N-5	1296	1382	5547	16,590	9864	5076	12,332	7365	2527	6575	6246	3080	7129	5858
N-6	1084	1458	2442	6054	3413	2839	5812	4149	1712	3332	3332	2033	3652	3652
N-7	354	611	511	3098	891	533	2717	738	400	1169	703	355	1124	658
N-11	1513	1513	2952	9788	4355	2845	12,625	3839	2196	7460	3492	2340	7604	3489
N-13	875	875	1409	2313	1691	1003	1448	1207	1095	1536	1352	1162	1603	1419
N-14	1209	1209	1422	2731	1697	1000	1866	1213	1094	1957	1352	1159	2021	1417
N-15	1995	1995	3330	7016	5746	2639	9654	3574	2053	5120	3358	1898	4965	3203
N-16	5680	8000	12,263	24,165	20,669	8596	28,799	11,698	5266	14,102	9690	5498	14,335	8915
N-19	1349	1349	2206	2313	2313	1427	1534	1534	1932	2039	2039	2350	2457	2457
N-20	2905	2925	6329	7655	7391	4365	5427	5427	3185	4246	4246	3840	4902	4902
N-21	2899	2920	4319	6469	4610	2825	3510	3510	2047	3698	3435	2445	4096	3711
N-22	1764	1764	1475	3278	2018	1214	1757	1730	949	1473	1473	1032	1556	1556
N-25	3195	3552	2058	5923	3093	2044	3326	2950	1725	3323	3323	2116	3713	3546
N-26	1666	1866	750	3164	1322	997	1573	1412	1120	2115	1996	1225	2220	1938
N-28	3453	5193	3499	7335	4573	1651	2343	2287	1846	2847	2847	2037	3038	3038
N-29	3581	4766	3448	7238	4523	1637	2329	2267	1830	2831	2830	2020	3020	3020
N-30	4517	6699	3448	7238	4523	1637	2329	2267	1830	2831	2830	2020	3020	3020
N-31	2394	2990	9455	16,382	13,558	7302	18,690	10,425	3928	9189	8784	4268	9529	7995

Load Test Information			Calculated Capacities (kips)											
Case ID	Nominal Resistance (kips)	Max. Applied Load (kips)	FHWA			USACE			REVISED LAMBDA			API		
			U	P	I	U	P	I	U	P	I	U	P	I
N-32	1651	1693	2241	3603	2475	2461	2695	2695	2894	3128	3128	3678	3912	3912
N-33	1551	1610	2784	4146	3018	3140	3374	3374	3871	4105	4105	4881	5115	5115
N-35	1618	1618	1479	5748	2493	2473	4490	3619	1620	3431	3431	1877	3688	3589
N-37	5793	6742	8953	21,296	14,985	6835	30,587	9180	5037	16,831	8172	5044	16,837	7454
N-38	7859	7859	10,556	13,548	12,141	6830	8415	8415	5692	7278	7278	6334	7919	7919
N-39	2254	2500	8709	15,027	9124	5526	5942	5942	3991	4407	4407	4501	4917	4917
N-40	5421	7191	9131	11,938	9644	5485	9107	7956	4392	14,013	8126	4486	14,107	7653
N-41	3200	3200	8212	18,485	14,201	6284	17,614	8936	3246	8831	7111	3825	9410	6904
N-42	3377	3975	6100	14,052	9199	3928	7929	5517	2631	5516	5516	3042	5927	5182
N-43	3351	4090	13,950	21,159	17,606	11,028	26,022	15,796	5869	13,610	13,104	5811	13,552	10,867
N-44	7725	8000	26,709	37,589	31,105	18,169	31,897	26,026	10,677	15,272	15,272	8992	13,587	13,587
N-45	6565	8045	10,048	19,095	16,500	6524	19,725	9038	3821	10,313	7492	4139	10,631	7105
N-46	834	845	1516	3040	2034	1127	2365	1454	1084	1947	1502	1155	2017	1572
N-47	1037	1037	1262	2602	1854	1041	1676	1434	1019	1636	1623	1091	1709	1677
N-48	1288	1288	1416	3022	1918	1068	2482	1438	1058	2186	1557	1164	2292	1652
N-49	1988	2029	2966	7445	4288	2349	3927	3282	1949	3677	3664	2340	4069	3873
N-51	1176	1436	1296	2517	1357	1363	1691	1691	1067	2213	1679	1351	2497	1913
N-52	1499	1499	919	3069	1218	1017	2155	1366	737	1649	1223	851	1763	1329
N-53	878	896	1378	2586	1439	1354	1717	1717	1046	2192	1689	1288	2434	1882
N-54	1148	1239	1181	7360	1803	1308	4801	1865	833	2897	1589	1001	3066	1757
N-55	1425	1456	742	4264	1127	702	2894	1017	555	1752	944	553	1750	942
N-56	3619	3619	1722	2069	2069	3179	3526	3526	2263	2610	2610	2625	2972	2972
N-57	1300	1300	1175	2635	1499	852	1997	951	489	1030	597	444	986	553

Load Test Information			Calculated Capacities (kips)											
Case ID	Nominal Resistance (kips)	Max. Applied Load (kips)	FHWA			USACE			REVISED LAMBDA			API		
			U	P	I	U	P	I	U	P	I	U	P	I
N-58	1350	1350	5211	6950	6141	3087	4903	4229	1619	2724	2724	1888	2992	2992
N-59	1545	1545	1950	2173	1989	1408	1447	1447	1285	1324	1324	1209	1248	1248
N-62	1431	1560	2166	2987	2723	2449	3868	3151	1400	2270	2190	1409	2279	2199
N-65	219	219	123	254	135	149	214	171	251	279	279	143	219	171
N-66	341	398	115	304	155	117	138	138	166	229	229	182	245	245
N-67	355	390	498	1935	577	499	575	575	1045	1167	1167	914	1037	1037
N-68	489	550	470	1812	550	481	557	557	985	1107	1107	874	997	997
N-69	88	180	19	116	34	62	110	92	54	84	84	54	84	84
N-70	163	180	19	181	31	38	88	56	41	71	71	43	88	73
N-71	876	933	161	911	232	238	440	333	228	346	346	250	475	369
N-72	600	627	161	911	232	238	440	333	228	346	346	250	475	369
N-73	484	487	608	2165	872	1015	1641	1289	775	1181	1181	821	1439	1225
N-74	800	800	345	2223	532	562	1262	784	415	776	776	462	1019	823
N-75	208	213	109	124	118	122	138	132	194	204	204	111	126	120
N-76	180	180	104	119	112	117	132	125	189	197	197	105	120	113
N-81	564	766	602	1163	712	591	737	694	529	672	672	648	963	782
N-82	161	184	18	66	31	50	73	72	74	100	100	65	92	92
N-84	440	440	540	540	540	462	462	462	537	537	537	508	508	508
N-85	594	594	990	990	990	795	795	795	927	927	927	1070	1070	1070
N-86	315	322	419	957	461	297	527	330	342	386	386	277	496	321
N-87	180	211	195	218	218	190	213	213	225	248	248	161	183	183
N-88	225	225	185	191	191	142	148	148	174	180	180	126	131	131
N-89	439	439	272	277	277	147	152	152	228	233	233	164	169	169

Load Test Information			Calculated Capacities (kips)											
Case ID	Nominal Resistance (kips)	Max. Applied Load (kips)	FHWA			USACE			REVISED LAMBDA			API		
			U	P	I	U	P	I	U	P	I	U	P	I
N-90	481	481	237	248	248	145	156	155	205	216	216	141	152	152
N-91	537	537	237	246	246	146	154	154	206	214	214	141	150	150
N-92	383	383	237	246	246	146	154	154	206	214	214	141	150	150
N-95	353	353	504	2317	680	536	727	685	954	1346	1346	1149	1541	1507
N-96	1697	1872	2604	2860	2652	1941	1989	1989	3578	3626	3626	3466	3514	3514
N-97	1542	1676	2014	2270	2062	1390	1439	1439	2195	2243	2243	2365	2413	2413

Appendix D. Calculated Capacities for the CPT Design Methods

Load Test Information			Calculated Capacities (kips)											
Case ID	Nominal Resistance (kips)	Max. Applied Load (kips)	NGI-04			ICP-05			FUGRO-04			UWA-05		
			U	P	I	U	P	I	U	P	I	U	P	I
N-8	1350	1597	972	1050	1050	671	687	687	658	840	766	668	707	697
N-9	5089	7194	6111	8667	8667	7452	9305	9305	7442	10,033	10,033	6306	11,783	8990
N-10	6417	8093	7815	10,588	10,588	8791	9709	9709	6348	8541	8541	6701	9411	8050
N-12	1245	1245	905	1089	1089	748	958	925	715	933	900	742	954	920
N-17	1046	1057	229	307	307	187	299	264	187	299	264	187	299	264
N-18	832	835	229	307	307	185	298	263	185	298	263	185	298	263
N-23	2717	3698	2289	3247	3247	2768	2926	2926	1467	2138	2138	2224	2751	2581
N-24	2952	4073	2287	3245	3245	2759	2918	2918	1443	2114	2114	2217	2744	2574
N-27	1660	2653	1880	1722	1722	2157	2157	2157	2101	2426	2426	2126	2789	2655
N-34	1477	1797	2974	3134	3134	6975	7348	7135	6770	7142	6929	6909	7281	7068
N-36	1171	1215	1360	1436	1436	912	1012	989	912	1012	989	912	1012	989

Load Test Information			Calculated Capacities (kips)											
Case ID	Nominal Resistance (kips)	Max. Applied Load (kips)	NGI-04			ICP-05			FUGRO-04			UWA-05		
			U	P	I	U	P	I	U	P	I	U	P	I
N-50	7324	7592	6349	8816	8816	7442	8974	8779	6656	9769	9574	6028	10,157	7886
N-60	1953	2109	1855	1193	1193	2014	1668	1668	2219	2629	2594	2088	1429	1429
N-61	746	932	897	679	679	1337	1343	1337	1289	1296	1071	1410	1417	1191
N-63	2844	2762	1891	1526	1526	2036	2186	2124	2401	3241	3018	2131	1897	1897
N-64	986	1214	956	898	898	1172	1172	1172	1277	1481	1481	1142	1009	1009
N-77	900	900	517	698	698	593	673	673	478	775	772	605	805	776
N-78	321	380	491	668	668	566	646	646	451	748	718	580	780	751
N-79	680	719	610	365	365	669	669	669	686	690	690	719	631	631
N-80	731	742	528	260	260	562	559	559	598	594	594	609	510	510
N-83	687	811	893	964	964	623	650	649	592	682	672	617	655	650
N-93	1096	1096	1175	1283	1283	1290	1347	1397	1290	1347	1397	1290	1347	1397
N-94	767	767	835	905	905	932	987	1002	932	987	1002	932	987	1002

References

1. Paikowsky, S. The Mechanism of Pile Plugging in Sand. In Proceedings of the All Days, OTC, Houston, TX, USA, 2–5 May 1990.
2. Paik, K.; Salgado, R. Determination of Bearing Capacity of Open-Ended Piles in Sand. *J. Geotech. Geoenvironmental Eng.* **2003**, *129*, 46–57. [[CrossRef](#)]
3. Raines, R.D.; Ugaz, O.G.; O'Neill, M.W. Driving Characteristics of Open-Toe Piles in Dense Sand. *J. Geotech. Eng.* **1992**, *118*, 72–88. [[CrossRef](#)]
4. Iskander, M. *Behavior of Pipe Piles in Sand: Plugging and Pore-Water Pressure Generation during Installation and Loading*, Springer Series in Geomechanics and Geoengineering; Springer: Berlin/Heidelberg, Germany, 2011.
5. Paik, K.; Lee, S. Behavior of soil plugs in open-ended model piles driven into sands. *Mar. Georesour. Geotechnol.* **1993**, *11*, 353–373. [[CrossRef](#)]
6. Smith, I.M.; Chow, Y.K. Three-dimensional analysis of pile drivability. In Proceedings of the 2nd International Conference on Numerical Methods in Offshore Piling, Austin, TX, USA, 18–22 May 1982; pp. 1–19.
7. Smith, I.M.; To, P.; Wilson, S.M. Plugging of pipe piles. In Proceedings of the 3rd International Conference on Numerical Method in Offshore Piling, Nantes, France, 21–22 May 1986; pp. 53–73.
8. Paikowsky, S.G.; Whitman, R.V.; Baligh, M.M. A new look at the phenomenon of offshore pile plugging. *Mar. Geotechnol.* **1989**, *8*, 213–230. [[CrossRef](#)]
9. Randolph, M.F.; Leong, E.C.; Houlsby, G.T. One-dimensional analysis of soil plugs in pipe piles. *Géotechnique* **1991**, *41*, 587–598. [[CrossRef](#)]
10. Randolph, M.; May, M.; Leong, E.; Hyden, A.M.; Murff, J.D. Soil Plug Response in Open-Ended Pipe Piles. *J. Geotech. Eng.* **1992**, *118*, 743–759. [[CrossRef](#)]
11. Choi, Y.; O'Neill, M.W. Soil Plugging and Relaxation in Pipe Pile during Earthquake Motion. *J. Geotech. Geoenvironmental Eng.* **1997**, *123*, 975–982. [[CrossRef](#)]
12. Murff, J.; Raines, R.; Randolph, M. Soil Plug Behavior of Piles in Sand. In Proceedings of the Offshore Technology Conference, Houston, TX, USA, 2–5 May 1990.
13. Miller, G.A.; Lutenecker, A.J. Influence of Pile Plugging on Skin Friction in Overconsolidated Clay. *J. Geotech. Geoenvironmental Eng.* **1997**, *123*, 525–533. [[CrossRef](#)]
14. Henke, S.; Grabe, J. Numerical investigation of soil plugging inside open-ended piles with respect to the installation method. *Acta Geotech.* **2008**, *3*, 215–223. [[CrossRef](#)]
15. Henke, S.; Grabe, J. Field measurements regarding the influence of the installation method on soil plugging in tubular piles. *Acta Geotech.* **2013**, *8*, 335–352. [[CrossRef](#)]
16. Randolph, M.F. Science and empiricism in pile foundation design. *Géotechnique* **2003**, *53*, 847–875. [[CrossRef](#)]
17. Brucy, F.; Meunier, J.; Nauroy, J.-F. Behavior of Pile Plug in Sandy Soils During and After Driving. In Proceedings of the Offshore Technology Conference, Houston, TX, USA, 6–9 May 1991.
18. Focht, J.A.; McClelland, B. Analysis of Laterally Loaded Piles by Difference Equation Solution. *Tex. Eng.* **1955**, *25*, 7–9.
19. Fattah, M.Y.; Al-Soudani, W.H. Bearing capacity of open-ended pipe piles with restricted soil plug. *Ships Offshore Struct.* **2015**, *11*, 1–16. [[CrossRef](#)]
20. Paikowsky, S.G.; Whitman, R.V. The effects of plugging on pile performance and design. *Can. Geotech. J.* **1990**, *27*, 429–440. [[CrossRef](#)]
21. Lehane, B.M.; Gavin, K.G. Discussion of “Determination of Bearing Capacity of Open-Ended Piles in Sand” by Kyuho Paik and Rodrigo Salgado. *J. Geotech. Geoenvironmental Eng.* **2004**, *130*, 656–658. [[CrossRef](#)]
22. Yu, F.; Yang, J. Base Capacity of Open-Ended Steel Pipe Piles in Sand. *J. Geotech. Geoenvironmental Eng.* **2012**, *138*, 1116–1128. [[CrossRef](#)]
23. Jeong, S.; Ko, J.; Won, J.; Lee, K. Bearing capacity analysis of open-ended piles considering the degree of soil plugging. *Soils Found.* **2015**, *55*, 1001–1014. [[CrossRef](#)]
24. De Nicola, A.; Randolph, M.F. The plugging behaviour of driven and jacked piles in sand. *Géotechnique* **1997**, *47*, 841–856. [[CrossRef](#)]
25. Lehane, B.; Randolph, M.F. Evaluation of a Minimum Base Resistance for Driven Pipe Piles in Siliceous Sand. *J. Geotech. Geoenvironmental Eng.* **2002**, *128*, 198–205. [[CrossRef](#)]
26. Petek, K.; Mitchell, R.; Ellis, H. *FHWA Deep Foundation Load Test Database Version 2.0 User Manual*; Report No. FHWA-HRT-17-034; U.S. Department of Transportation Federal Highway Administration: McLean, VA, USA, 2016.
27. Dennis, D.N.; Olson, R.E. Axial Capacity of Steel Pipe Piles in Clay. In Proceedings of the Conference on Geotechnical Practice on Offshore Engineering, Austin, TX, USA, 27–29 April 1983; pp. 370–388.
28. Dennis, N.D.; Olson, R.E. Axial capacity of steel pipe piles in sand. In Proceedings of the Geotechnical Practice in Offshore Engineering, Austin, TX, USA, 27–29 April 1983; pp. 389–402.
29. Olson, R.E.; Shantz, T.J. Axial Load Capacity of Piles in California in Cohesionless Soils. In *Current Practices and Future Trends in Deep Foundations*; American Society of Civil Engineers: Reston, VA, USA, 2004; pp. 1–15.
30. Iskander, M.; Garlanger, J.E.; Hussein, M.H. From Soil Behavior Fundamentals to Innovations in Geotechnical Engineering. In *Geo-Congress 2014 Technical Papers*; American Society of Civil Engineers: Reston, VA, USA, 2014; pp. 209–220.

31. Machairas, N.; Highley, G.A.; Iskander, M.G. Evaluation of FHWA Pile Design Method against the FHWA Deep Foundation Load Test Database Version 2.0. *Transp. Res. Rec. J. Transp. Res. Board* **2018**, *2672*, 268–277. [[CrossRef](#)]
32. ASTM International. *D18 Committee Test Methods for Deep Foundations under Static Axial Compressive Load*; D1143; ASTM International: West Conshohocken, PA, USA, 2018.
33. Naval Facilities Engineering Command. *Design Manual 7.01 (DM-7.01) Soil Mechanics*; NAVFAC: Alexandria, VA, USA, 1986.
34. Peck, R.B.; Hanson, W.E.; Thornburn, T.H. *Foundation Engineering*, 2nd ed.; John Wiley and Sons: New York, NY, USA, 1974.
35. Rizk, A.; Machairas, N.; Iskander, M. Evaluation of Several Design Methods for Calculating Axial Compression Capacity of Large Diameter Open-Ended Piles. In Proceedings of the IFCEE 2021, Dallas, TX, USA, 12–14 May 2021; pp. 98–107.
36. Hannigan, P.J.; Rausche, F.; Likins, G.E.; Robinson, B.; Becker, M.; Berg, R.R. *Design and Construction of Driven Pile Foundations—Volume I (No. FHWA-NHI-16-009)*; National Highway Institute (US): Washington, DC, USA, 2016.
37. U.S. Army Corps of Engineers (USACE). *Design of Pile Foundations*; Engineer Manual 1110-2-2906; U.S. Army Corps of Engineers (USACE): Washington, DC, USA, 1991.
38. Focht, J.A.; Vijayvergiya, V. A New Way to Predict Capacity of Piles in Clay. In Proceedings of the Offshore Technology Conference, Houston, TX, USA, 1–3 May 1972.
39. Kraft, L.M., Jr.; Focht, A., Jr.; Amerasinghe, S.F. Friction Capacity of Piles Driven into Clay. *J. Geotech. Eng. Div.* **1981**, *107*, 1521–1541. [[CrossRef](#)]
40. American Petroleum Institute. *API Recommended Practice for Planning, Designing, and Constructing Fixed Offshore Platforms, Report RP-2A*; American Petroleum Institute, Production Department: Washington, DC, USA, 1993.
41. Reese, L.C.; Isenhower, W.M.; Wang, S. *Analysis and Design of Shallow and Deep Foundations*; Wiley: Hoboken, NJ, USA, 2005; Volume 10.
42. Wang, S.T.; Arrellaga, J.A.; Vasquez, L. *APILE v2019—Technical Manual: A Program for the Study of Driven Piles under Axial Loads*; ENSOFT: Austin, TX, USA, 2019.
43. Tomlinson, M.J. *Foundation Design and Construction*, 4th ed.; Pitman Advanced Publishing Program: Boston, MA, USA, 1980; p. 793.
44. Nordlund, R.L. Bearing Capacity of Piles in Cohesionless Soils. *J. Soil Mech. Found. Div.* **1963**, *89*, 1–35. [[CrossRef](#)]
45. Pelletier, J.; Murff, J.; Young, A. Historical Development and Assessment of the Current Api Design Methods For Axially Loaded Pipes. In Proceedings of the Offshore Technology Conference, Houston, TX, USA, 3–7 May 1993.
46. Murff, J.D. Pile capacity in a softening soil. *Int. J. Numer. Anal. Methods Géoméch.* **1980**, *4*, 185–189. [[CrossRef](#)]
47. Kodsy, A.; Machairas, N.; Iskander, M.G. Assessment of Several Interpreted Pile Capacity Criteria for Large-Diameter Open-Ended Piles. *Geotech. Test. J.* **2021**, *44*. [[CrossRef](#)]
48. Kodsy, A.; Iskander, M.; Machairas, N. Assessment of Several Nominal Resistance Interpretation Criteria for Drilled Foundations. *J. Geotech. Geoenvironmental Eng.* **2022**, *148*, 04021181. [[CrossRef](#)]
49. Rizk, A.; Kodsy, A.; Machairas, N.; Iskander, M. Efficacy of Design Methods for Predicting the Capacity of Large Diameter Open-Ended Piles. *J. Geotech. Geoenviron. Eng.* **2022**. *in Press*.
50. Ko, J.; Jeong, S. Plugging effect of open-ended piles in sandy soil. *Can. Geotech. J.* **2015**, *52*, 535–547. [[CrossRef](#)]
51. Suits, L.D.; Sheahan, T.C.; Iskander, M. On the Design of Instrumented Double-Wall Model Piles Used to Investigate Plugging of Open-Ended Pipe Piles. *Geotech. Test. J.* **2011**, *34*, 147–154. [[CrossRef](#)]
52. Aas, P.; Karlsrud, K.; Clausen, C. Bearing capacity of driven piles in sand, the NGI approach. In Proceedings of the Frontiers in Offshore Geotechnics, Perth, Australia, 19–21 September 2005.
53. Aas, P.; Karlsrud, K.; Clausen, C. Bearing capacity of driven piles in clay, the NGI approach. In Proceedings of the Frontiers in Offshore Geotechnics, Perth, Australia, 19–21 September 2005; Volume 1, pp. 775–782.
54. Jardine, R.; Chow, F.; Standing, J.; Overy, R. *ICP Design Methods for Driven Piles in Sands and Clays*; Thomas Telford Ltd.: London, UK, 2005.
55. Kolk, H.J.; Baaijens, A.E.; Senders, M. Design criteria for pipe piles in silica sands. In Proceedings of the International Symposium on Frontiers in Offshore Geomechanics (ISFOG 2005), Perth, Australia, 19–21 September 2005.
56. Schneider, J.; Lehane, B.; Xu, X. The UWA-05 method for prediction of axial capacity of driven piles in sand. In Proceedings of the International Symposium on Frontiers in Offshore Geomechanics (ISFOG 2005), Perth, Australia, 19–21 September 2005; pp. 683–689.
57. Kikuchi, Y.; Mizutani, M.; Yamashita, H. Vertical bearing capacity of large diameter steel pipe piles. In *Advances in Deep Foundations*; CRC Press: Boca Raton, FL, USA, 2007; pp. 189–194.
58. Han, F.; Ganju, E.; Prezzi, M.; Salgado, R.; Zaheer, M. Axial resistance of open-ended pipe pile driven in gravelly sand. *Géotechnique* **2020**, *70*, 138–152. [[CrossRef](#)]
59. Liu, J.-W.; Zhang, Z.-M.; Yu, F.; Xie, Z.-Z. Case History of Installing Instrumented Jacked Open-Ended Piles. *J. Geotech. Geoenvironmental Eng.* **2012**, *138*, 810–820. [[CrossRef](#)]
60. Tveldt, G.; Fredriksen, F. E18 Ny motorvegbru i Drammen. Prøvebelastning av peler. In Proceedings of the Conference on Rock Blasting and Geotechnics, Sandton, South Africa, 10–13 September 2003.
61. Jardine, R.J.; Standing, J.R. *Pile Load Testing Performed for HSE Cyclic Loading Study at Dunkirk, France. V. 1. Technical Report*; Health and Safety Executive: Bootle, UK, July 2000.

62. Williams, R.E.; Chow, F.C.; Jardine, R.J. Unexpected behaviour of large diameter tubular steel piles. In Proceedings of the International Conference on Foundation Failures, Singapore, 12–13 May 1997; pp. 363–378.
63. Yang, Z.X.; Guo, W.B.; Zha, F.S.; Jardine, R.J.; Xu, C.J.; Cai, Y.Q. Field Behavior of Driven Prestressed High-Strength Concrete Piles in Sandy Soils. *J. Geotech. Geoenvironmental Eng.* **2015**, *141*, 04015020. [[CrossRef](#)]
64. Mayne, P.W.; (Georgia Institute of Technology, Atlanta, GA USA) FHWA Deep Foundation Load Test Database (DFLTD). Personal communication, 2013.
65. Petek, K.A.; Mitchell, R.A.; Buechel, G.J.; Goodyear, D. Full Scale Instrumented Pile Load Test for the Port Mann Bridge, Surrey, British Columbia, Canada. In *Full-Scale Testing and Foundation Design*; American Society of Civil Engineers: Reston, VI, USA, 2012; pp. 362–375.
66. Gilchrist, J.M. Load Tests on Tubular Piles in Coralline Strata. *J. Geotech. Eng.* **1985**, *111*, 641–655. [[CrossRef](#)]
67. Wilbur Smith Associates. *Report on Pile Load Test PROGRAM (LA-1 Improvements)*; Final Report to Louisiana Department of Transportation; Louisiana Department of Transportation: Baton Rouge, LA, USA, 2004.
68. McVay, M.C.; Badri, D.; Hu, Z.Y. *Determination of Axial Pile Capacity of Prestressed Concrete Cylinder Piles*; No. UF Proj 4910-4504-877-12; University of Florida: Tallahassee, FL, USA, 2004.
69. Matsumoto, T.; Michi, Y.; Hirano, T. Performance of Axially Loaded Steel Pipe Piles Driven in Soft Rock. *J. Geotech. Eng.* **1995**, *121*, 305–315. [[CrossRef](#)]
70. Cox, W.R.; Solomon, I.J.; Cameron, K. Instrumentation and calibration of two 762 mm diameter pipe piles for axial load tests in clays. In *Large-Scale Pile Tests in Clay*; Thomas Telford: Telford, UK, 1993; pp. 217–236.
71. Pump, W.; Korista, S.; Scott, J. Installation and load tests of deep piles in Shanghai alluvium. In Proceedings of the 7th International Conference on Piling and Deep Foundations, Vienna, Austria, 15–17 June 1998; pp. 31–36.
72. Kusakabe, O.; Mitsumoto, T.; Sandanbata, I.; Kosuge, S.; Nishimura, S. Predictions of bearing capacity and driveability of piles. In Proceedings of the International Conference Soil Mechanics and Foundation Engineering, ISSMFE, Rio de Janeiro, Brazil, 13–18 October 1989; Volume 5, p. 2957.
73. Bradshaw, A.S.; Haffke, S.; Baxter, C.D.P. Load Transfer Curves from a Large-Diameter Pipe Pile in Silty Soil. In *Full-Scale Testing and Foundation Design*; American Society of Civil Engineers: Reston, VI, USA, 2012; pp. 590–601.
74. Robertson, P.K.; Campanella, R.G.; Brown, P.T.; Grof, I.; Hughes, J.M.O. Design of axially and laterally loaded piles using in situ tests: A case history. *Can. Geotech. J.* **1985**, *22*, 518–527. [[CrossRef](#)]
75. Richard, L. *Spiral Welded Pipe Piles for Structures in Southeastern Louisiana*. Unpublished. Doctoral Dissertation, University of New Orleans, Louisiana, OR, USA, 2010.
76. Caltrans. *I-880 5th St. Overhead Bent 16, Br. No:133-01, CT-ID:133-01*; California Department of Transportation: Sacramento, CA, USA, 2014.
77. Liebich, B.A. High-Capacity Piles at the Stony Creek Bridge Project. *Transp. Res. Rec. J. Transp. Res. Board* **2009**, *2116*, 41–46. [[CrossRef](#)]
78. Ta, J.L.; Liebich, B.A. *Pile Dynamic Analysis and Pile Load Test Results: Test Pile at Pier 12, Feather River Bridge 18-0026R*; Foundation Testing Branch, California Department of Transportation: Sacramento, CA, USA, 2011.
79. Caltrans. *Route 101 Hum Pier 2L, Br. No: 04-0025L, CT-ID:136-01*; California Department of Transportation: Sacramento, CA, USA, 2009.
80. Caltrans. *Russian River Route 120 Abutment 11, Br. No: 10-0301, CT-ID: 138-01*; California Department of Transportation: Sacramento, CA, USA, 2015.
81. Caltrans. *Russian River Route 222, Br. No:10-0301, CT-ID:137-01*; California Department of Transportation: Sacramento, CA, USA, 2015.
82. Mercea, C.; Awad, Y.M. *Pile Field Acceptance Criteria, Pile Dynamic Analysis, and Pile Load Test Results: Test-Pile at Bent 3, Santa Clara River Bridge 53-2925*; Foundation Testing Branch, California Department of Transportation: Sacramento, CA, USA, 2002.
83. Caltrans. *Port of Oakland conn. Via. No. 33-0612E Bents: 10NCI, 17NCI, 27NC.; Br. No.: 33-612; CT-IDs: 012-05/06, 012-03/04, 012-05/06*; California Department of Transportation: Sacramento, CA, USA, 2002.
84. Brzezinski, L.S.; Baba, H.U. Offshore Open End Steel Tubular Piles-A Case History. In *Full-Scale Testing and Foundation Design*; American Society of Civil Engineers: Reston, VI, USA, 2012; pp. 568–589.
85. Shioi, Y.; Yoshida, O.; Meta, T.; Homma, M. Estimation of bearing capacity of steel pipe pile by static loading test and stress-wave theory (Trans-Tokyo Bay Highway). In Proceedings of the International Conference on the Application of Stress-Wave Theory to Piles, The Hague, The Netherlands, 21–24 September 1992; pp. 325–330.
86. Greiner Engineering Sciences. *Load Tests Report: L.R. 795 Section B-6*; Commonwealth of Pennsylvania, Department of Transportation: Philadelphia, PA, USA, 1982.
87. Ishihara, K.; Saito, A.; Shimmi, Y.; Miura, Y.; Tominaga, M. Blast Furnace Foundation in Japan. In Proceedings of the Ninth International Conference on Soil Mechanics and Foundation Engineering, Tokyo, Japan, 1977; pp. 157–236. Available online: https://www.issmge.org/uploads/publications/1/35/1981_04_0008.pdf (accessed on 1 March 2022).
88. Load Testing of 14, in. *Square and 54 in. dia. Cylindrical Prestressed Concrete Piles at Crossbay Blvd. over North Channel*; Queens County. New York Department of Transportation (NYDOT): Albany, NY, USA, 1996.
89. McCammon, N.R.; Golder, H.Q. Some Loading Tests on Long Pipe Piles. *Géotechnique* **1970**, *20*, 171–184. [[CrossRef](#)]

90. Toğrol, E. Bearing capacity by load tests. *Int. J. Rock Mech. Min. Sci. Géoméch. Abstr.* **1975**, *12*, 101. [[CrossRef](#)]
91. Cox., W.; Kraft, L.M.; Verner, E. Axial Load Tests on 14-inch Pipe Piles in Clay. In Proceedings of the Offshore Technology Conference, Houston, TX, USA, 30 April–30 May 1979; pp. 1147–1158.
92. Heerema, E. Pile Driving And Static Load Tests On Piles In Stiff Clay. In Proceedings of the Offshore Technology Conference, Houston, TX, USA, 30 April–30 May 1979.